APPLYING CFD ANALYSIS TO PREDICTING ASFM BIAS IN LOW HEAD INTAKES WITH DIFFICULT HYDRAULIC CONDITIONS

D.D. Lemon, L. Bouhadji, J. Jiang †, D. Topham ‡
†ASL Environmental Sciences Inc, Sidney, BC, Canada.
‡Topham Scientific Consulting Services, Victoria, BC, Canada
dlemon@aslenv.com, lbouhadji@aslenv.com, jjiang@aslenv.com, topham@telus.net

Abstract

Turbulent flows in a powerhouse intake are investigated using computational fluid dynamics. Some intakes present severe hydraulic conditions, with strong spatial variations in both the mean flow and the turbulence. Such conditions can make determining an appropriate sampling strategy difficult for any instrument measuring intake flows. It can also, in some cases, cause systematic errors in Acoustic Scintillation Flow Meter (ASFM) velocity measurements. Successful numerical modelling of the flow in the intake can be used to plan a measurement program. The numerical model can also be used to estimate bias, which may occur in ASFM measurements as a result of such difficult conditions. The performance of the CFD model is examined for a particular intake by comparing the modelled mean flow with data from an ASFM and the computed turbulent kinetic energy with measurements from a Doppler velocimeter mounted in the intake.

Introduction

ASL has developed the non-intrusive Acoustic Scintillation Flow Meter (ASFM) for monitoring velocities and total flows in the intakes of low head hydroelectric plants. These measurements allow hydro engineers to evaluate turbine operation efficiency and quantify changes in turbine performance from changes in the intake, such as the use of fish protection devices within the intake. The basic operation of the ASFM system can be found in the paper by Lemon, Billenness and Lampa (2002).

Low-head intakes present one of the most difficult configurations in which to make accurate measurements of turbine discharge. The most difficult examples combine the short distance

[1]Presented at the 5^{th} International Group Innovation in Hydraulic Efficiency Measurement Conference, Lucerne, Switzerland, July 2004.

between the entrance and the turbine and the converging cross-section of the water passage with significant upstream obstructions in the form of trash-rack support beams, large members in the trash-rack or fish diversion screens. Oblique entrance flows can further complicate the situation. Such conditions can produce irregular distributions of velocity and turbulence in the intake, which may produce significant biases in the velocity measured by an ASFM. When the deployment of the ASFM in a more favourable location is difficult or impossible, CFD simulation of the intake flow and turbulence fields can be used to estimate the bias in the ASFM measurements. CFD simulations rely on engineering models to approximate the turbulence in the simulated flow, since it is not presently feasible to simulate the full instantaneous velocity field. The accuracy with which potential ASFM bias can be forecast using a simulation depends on the accuracy with which the turbulence and mean velocity fields can be computed. Direct measurements of the velocity turbulence were therefore collected in an intake for comparison with the turbulent kinetic energy calculated in a simulation of the intake flow.

In this paper, a three-dimensional simulation in the Hydro-Kennebec powerhouse intakes (Maine, USA) is presented and compared with direct measurements of both the velocity and turbulence fields in the intake. An unstructured, parallel code is used to solve the discretized Navier-Stokes equations with a shear stress transport (SST) based $k-\omega$ turbulence model. All the simulations were performed on ASL's parallel computing facility. The CFD results are compared to the Acoustic Scintillation Flow Meter (ASFM) and Nortek Doppler Velocimeter (NDV) data collected by ASL-AQFlow at Hydro-Kennebec in June 2003.

1 Numerical implementation

The numerical simulations are performed using the unstructured, parallel solver CFX 5.6 and the mesh is generated by using ICEM-CFD hexa. Both codes are from Ansys Inc. The governing differential equations are integrated over control volumes defined by the grid, such that the relevant quantity (mass, momemtum, energy) is conserved in a discrete sense for each control volume. The diffusive and advective fluxes and the source terms in the volume integrals are then discretized using various techniques. The discretization method must be selected to ensure both adequate accuracy and numerical stability. For the advection terms, CFX 5.6 provides three different schemes: a first order Upwind Differencing Scheme (UDS), a numerical advection correction scheme and a high resolution scheme. The first order UDS is very robust (numerically stable) but suffers from numerical diffusion and is used usually as a first step to get an initial fluid flow solution before applying a higher resolution scheme. In the numerical advection correction scheme, one can specify a blend factor between 0 and 1 to fix a level of accuracy. A blend factor of 0 is equivalent to the first order advection scheme and a blend factor of 1 uses second order differencing which is more accurate but less robust. One can start a complex simulation by using a blend factor of 0 and gradually increase it towards 1. Usually a blend factor of 0.75 is sufficient. The high resolution scheme computes the blend factor throughout the domain based on the local solution field. In flow regions where variable gradients are low, the blend factor will be close to 1. In flow regions where variable gradients are sharp, the blend factor will be close to 0 to maintain robustness.

The high resolution scheme was selected for the present study as a first step and a blend factor of 1 was selected in a final calculation. No difference has been found between using a blend factor of 1 and the high resolution scheme (in regions of interest).

2 Turbulence modelling

Resolution of the instantaneous fluctuating flowfield in turbulent flows is not feasible for complex flows. Engineering methods implemented in CFD rely on the numerical solution of the Reynolds-averaged Navier-Stokes (RANS) equations in conjunction with turbulence models of varying degrees of complexity, ranging from algebraic eddy viscosity to Reynolds stress models. In the eddy viscosity models, such the basic $k-\varepsilon$, the RNG $k-\varepsilon$ or the $k-\omega$ models, the Reynolds stresses are linearly related to the mean velocity gradients in a fashion similar to the relationship between the stress and strain tensors in laminar Newtonian flows. In Reynolds stress turbulence models (RSM), the eddy viscosity hypothesis is not invoked. Instead, a transport equation is defined for each component of the Reynolds stress tensor. This model provides a conceptually more correct representation of turbulence characteristics such as anisotropy and the effect of extra strains, but is computationally intensive and difficult to converge in complex configurations.

As a result of the substantially lower computational effort required, the $k-\varepsilon$ model is still one of the most commonly used turbulence models for the solution of practical engineering flows. There is, however, a large amount of evidence that though the $k-\varepsilon$ model reproduces qualitatively many of the important flow features, it is not totally satisfactory in some complex flow situations, particularly those involving flow separation. In this work, the shear stress transport (SST) based $k-\omega$ turbulence model has been used. This model is designed to give a highly accurate prediction of flow separation under adverse pressure gradients. All the solid walls are treated with the scalable wall functions.

3 Computational domain and boundary conditions

The Hydro-Kennebec reservoir, intakes, turbine sections and cylindrical cross-members are shown in Figures 1 and 2. The power plant consists of two units: Unit 1, where a large inlet curvature (7.315 m radius) leads into the straight intake and Unit 2 where a straight wall is present prior to the entrance. Both units, separated by a 1.83 m wall, are 15.4 m high at the intake entrance and 7.036 m wide. The trash rack consists of five thick 0.25m x 0.69m I-beams, forty 1.27cm x 13.97cm vertical bars and thirty six 1.27cm x 2.54cm horizontal bars. Due to their small thickness, the bars are not included in the computational domain. The semi-circular front section of the turbines has a 2.97 m diameter. The origin O_{xyz} of the coordinate system is located on the bottom part of the trash rack as shown in Figure 1. The cylindrical cross members supporting the frames on which the acoustic transducers are mounted are located at a distance x=9.34 m. The ASFM plane of measurement is located upstream of the cylindrical pipes, at x=9 m. The distance between the ASFM plane and the turbine section is 1.536 m. More than 3.7 million nodes are used to grid the configuration.

The parallel computations are run in a cluster of three computers. A symmetry boundary condition is applied on the top plane of the reservoir. The remaining surfaces are walls.

The mean velocity distribution at the inlet boundaries was provided by the large scale ASL-COCIRM 3D numerical model of the forebay and is illustrated in Figure 3. ASL-COCIRM is a fully three-dimensional, finite difference and free surface hydrodynamic model. In this implementation, the model domain covers the entire forebay area of 302.4 m by 388.8 m. The domain was resolved using horizontal grids of size 1.8 m by 1.8 m and 16 equally-spaced sigma vertical layers. The upstream boundary conditions for the forebay were given by water surface elevations. The downstream boundary is located at the intakes of the turbines and the discharge through each turbine was specified. Since the upper boundary of the forebay model is defined as a free surface, the submerged curved roofline of the intake cannot be directly simulated. The effect of these curved boundaries in directing the flow into the intake has therefore been simulated by blocking the flow between the free surface of the model and the roofline with a series of vertical barriers. This directs the flow in such a manner as to give realistic approach conditions at the CFD model boundaries. For each model run, starting from the initial condition of zero velocities and a flat water surface, the detailed flows at the CFD boundaries were tabulated after the model results had converged to a stable state.

4 Direct Turbulence Measurements

As one of the prime sources of systematic error in the ASFM appears to be the distribution of turbulence and velocity in the wakes from major structural members in the trashrack, the field measurements were designed to sample the velocity and turbulence variation through one of those wakes. The largest structural members in the Kennebec intake were the five horizontal I-beams (69 cm deep in the along-stream direction, and 25 cm high). The wake profile could therefore be sampled by traversing an instrument along a vertical path in the intake. Direct measurement of all three components of the fluctuating velocity field requires the use of a rapid-sampling current meter, capable of being deployed in a hydroelectric intake. Acoustic velocimeters are the only instruments suitable for making such measurements under field conditions. In this case, the Nortek 10 MHz Field Velocimeter (NDV) was chosen. Figure 4 shows the components of the NDV. The unit used at Kennebec was equipped with a side-looking (right-angled) sensor head. The velocity measurement is taken in a sensing volume centred 5 cm in front of the central transducer face. The NDV operating parameters are listed below in Table 1.

The instrument was mounted on the bottom crossbar of the frame supporting the ASFM transducers, as shown in the diagram and photographs in Figure 5. The sensing head was positioned 1.74 metres from the left-hand side of the intake (looking in the direction of the flow), and 1.43 metres above the bottom of the frame's sidepieces. The support structure had fairing attached to reduce vibration from vortex-shedding. A detailed profile through one of the wakes was made by raising the frame to move the NDV head from 3.2 m to 4.9 m elevation in 10 cm increments in the intake to Unit 1. At each level, a 4-minute time series was collected; the turbine operating conditions were held constant throughout the hour and 45 minutes required to collect the profile. The mean velocity components U, V,

Table 1: NDV Operating Parameters.

Acoustic Frequency	**10 MHz**
Velocity range	**2.5 m/s**
Velocity resolution	**1 mm/s**
Sampling rate	**25 Hz**
Sampling Volume	**0.25 to 1** cm^3
Power Requirements	**125 mA @ 24VDC**
Communication and Data Output	**RS422**

and W and the corresponding variances u^2, v^2, and w^2 were computed from the time series at each elevation. The turbulent kinetic energy was then calculated as $K = (u^2+v^2+w^2)/2$. Figure 6 shows the profiles of U, K and the Reynolds stress through the wake. The profile begins in the centre of one wake, and ends at the beginning of the next. As expected, the turbulent kinetic energy has its maximum at the centre of the wake, and its minimum in the region between wakes. The Reynolds stress peaks at the edge of the wake. Figure 7 shows the spectrum of the velocity magnitude at the centre of the wake; the spectrum falls off with a -5/3 slope, consistent with the presence of an inertial subrange.

5 CFD Results

The simulation was undertaken with a discharge equal to 58.82 m^3/s through Unit 1 and 113.21 m^3/s through Unit 2. The discharge in Unit 2 was estimated by the operator when measurements were collected in Unit 1.

Figure 8 shows a comparison of the mean velocity magnitude (in the (x,y) plane) profile calculated by the model with the ASFM data in Unit 1. The agreement is found to be very good. The distribution of the mean velocity components and turbulent kinetic energy at selected (x,y) planes in Unit 1 is shown in Figure 9. The longitudinal section Z=-1 m corresponds to the section between the side wall and the turbine section in Unit 1 (1 meter away from the side wall). Large wakes are produced by the top I-beams as the flow comes down to the intake. These wakes diffuse, interact and merge by the slot location. Figures 10 and 11 show the same quantities in the ASFM plane of measurement ((y,z) plane) and in a horizontal section ((x,z) plane) for both units. The effect of the turbine section on the flowfield is clearly noticeable. The flow slows down over a large middle area when approaching the turbine nose whose diameter is 2.97 m ($\sim$40% of the intake cross section width). Large flow recirculations are present at the intake entrance to Unit 2. The velocity vectors at the ASFM plane of measurement, at selected elevations, are also shown in Figure 10. The flow is found to be steeper near the side walls of Unit 2. When approaching the turbine section, the flow slows down, the pressure increases and the flow is sucked up into the gate slot.

Figure 12 shows a comparison of the velocity components, the flow direction in degrees and

the turbulent kinetic energy with the local NDV measurements. The NDV measurements were collected in Unit 1 at the ASFM plane of measurement, in a vertical line between Y=3.2 and 5 m. This line is 1.74 m away from the wall, at Z=-5.3 m (see Figure 1). The flow rate in this particular case was not monitored by the ASFM system but was estimated to be close to 58 m^3/s. This difference in flow explains the small differences in magnitude for the velocity field and flow direction. The modelled mean turbulent kinetic energy shows a lower magnitude by a factor of 2, although a similar spatial distribution is obtained. This is likely the result of a turbulence background produced by the fine members which are not included in the CFD model or the ambient turbulence in the incoming flow, which is not included in the model either. Note also that the distribution of turbulent kinetic energy among the components is not equal; the w and u components show little variation through the wake and are almost equal; the increase in energy is nearly all in the v component, i.e. transverse to both the obstruction and the horizontal mean flow.

5.1 Conclusion

A three dimensional numerical analysis of turbulent flow in Hydro-Kennebec power plant intakes has been carried out. The configuration included a complex geometry involving trash racks, turbine sections, large curved sections and circular pipes as well as complex flow conditions at the inlet entrance such as a turning flow and separation. The CFD results show a good agreement with the integrated ASFM velocity magnitude and the local NDV mean velocity components. The turbulent kinetic energy magnitude is, however, lower than that found by the NDV measurements, although its variation with position agrees with the measured change. The discepancy is likely be related to the fine members of the trash rack which are not included in the model. The fine members are likely to increase the turbulence background within the intake, accounting for the offset between the measured and modelled turbulence levels.

The CFD simulation's agreement with the measured mean flow and the spatial distribution of the turbulent kinetic energy demonstrates its potential as a tool for estimating ASFM bias in intakes with difficult hydraulic conditions.

Acknowledgements

This work was partly supported by the Natural Sciences and Engineering Research Council of Canada (NSERC). The authors wish to thank the staff of the Kennebec hydroelectric plant for their help in the field measurements.

References

L. Bouhadji, D. Lemon, D. Topham, D. Billeness and D. Fissel, *CFD Analysis of Turbulent Flows In Hydroelectric Plant Intakes: Application to ASFM Technology*, Waterpower XIII conference, Buffalo, New York USA, July 29-31, 2003.

D.D. Lemon, D. Billenness and J. Lampa, *Recent advances in Estimating Uncertainties in Discharge Measurements with the ASFM*, Proceedings of the Hydro 2002 (Development, Management Performance) Conference, Kiris, Turkey, November, 2002. Published by International Journal of Hydropower & Dams, Aqua-Media Intl., Sutton, Surrey, U.K.

D.D. Lemon, L. Bouhadji, D.R. Topham, *Analysis of the Absolute Accuracy of ASFM Flow Measurements at Hydro-Kennebec*, Confidential report submitted to Delta Power Services, Winslow, Maine, USA, January 2004.

L. Bouhadji, *Three Dimensional CFD Study in Hydro-Kennebec Powerplant Intakes*, Internal technical report, ASL Environmental Sciences Inc., Sidney, BC, Canada, November 2003.

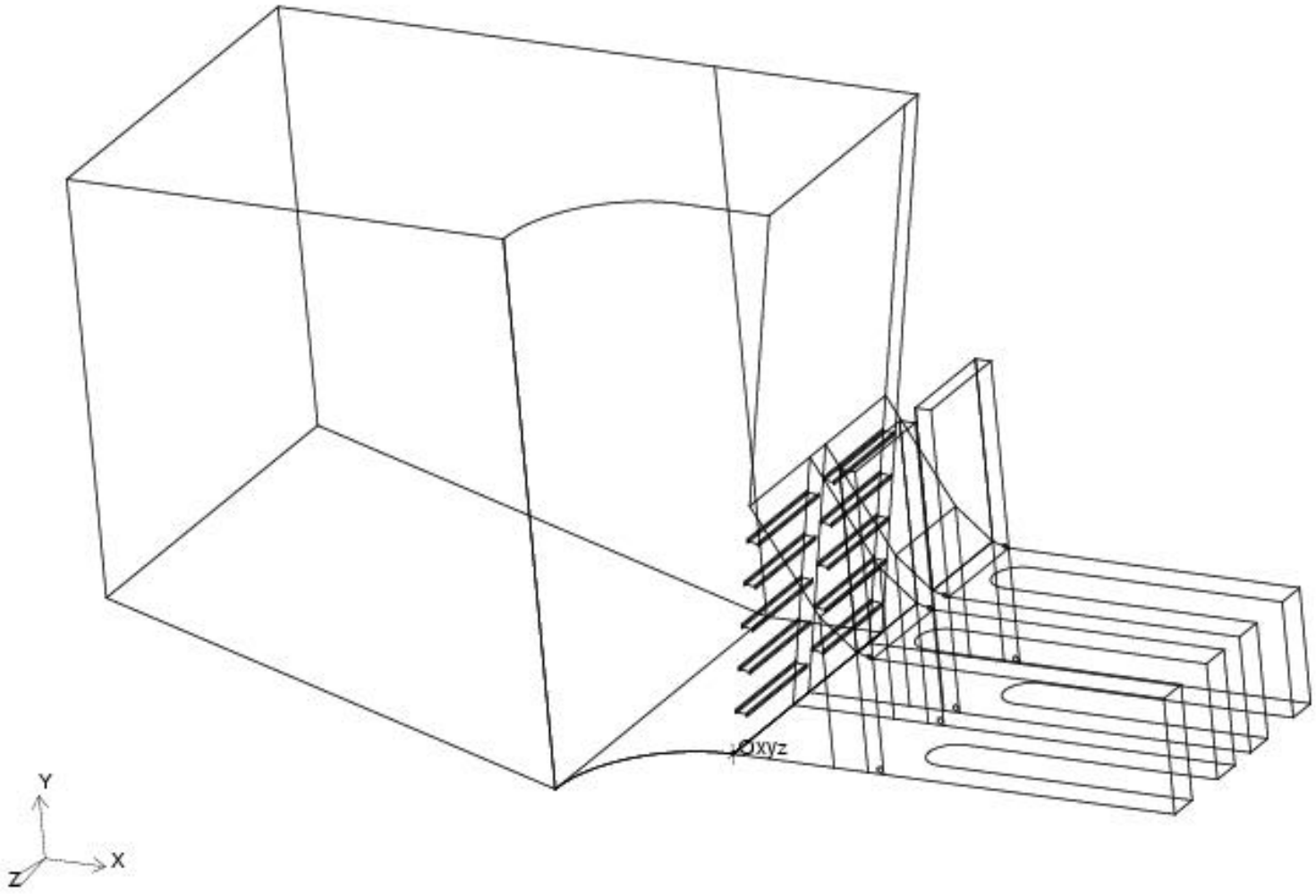

Figure 1: 3D Hydro-Kennebec intake frame.

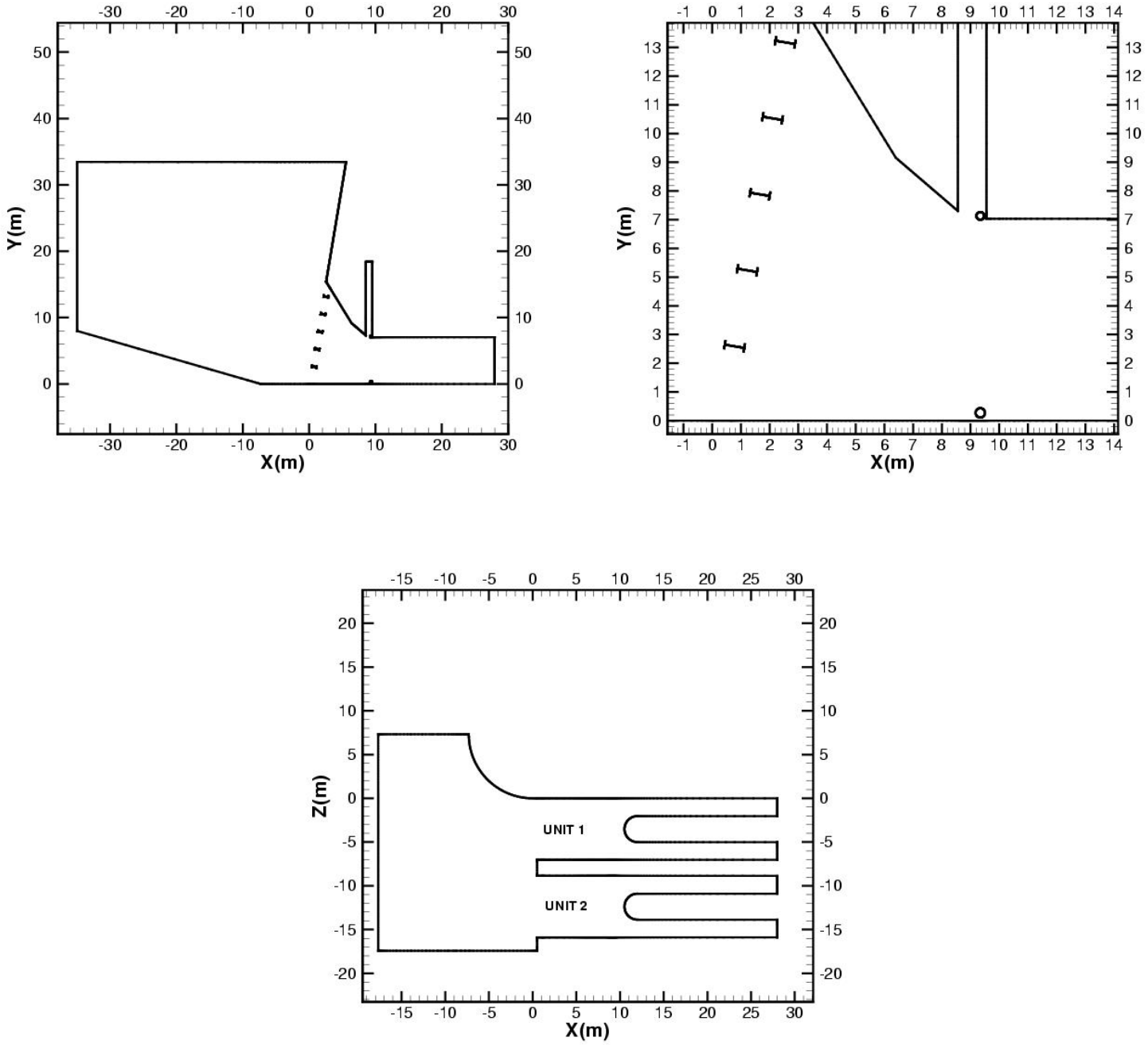

Figure 2: Selected longitudinal and lateral sections.

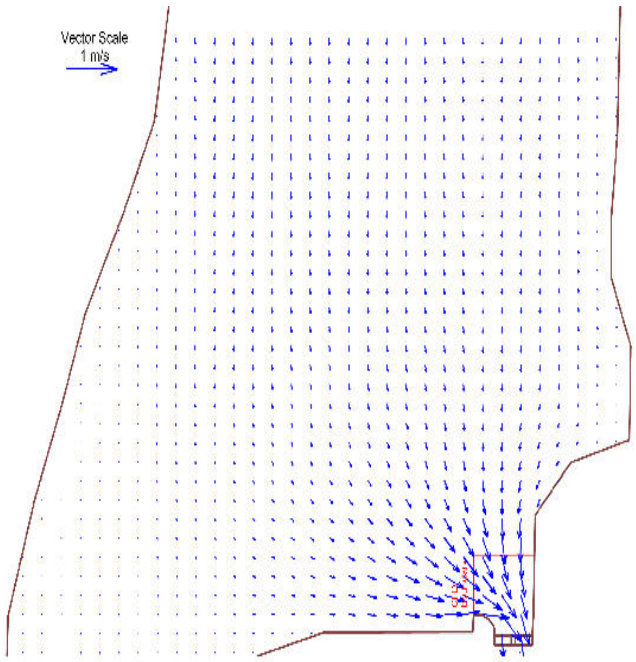

Figure 3: Distribution of the velocity vector at selected elevation in the forebay as computed by ASL-COCIRM numerical model. The inlet boundaries of the CFD computational domain are represented in red color.

Figure 4: Laboratory version of the ADV. As used at Kennebec, it was equipped with a right-angled head (inset), and the processor board was enclosed in a pressure case, connected to the surface by a power and communication cable.

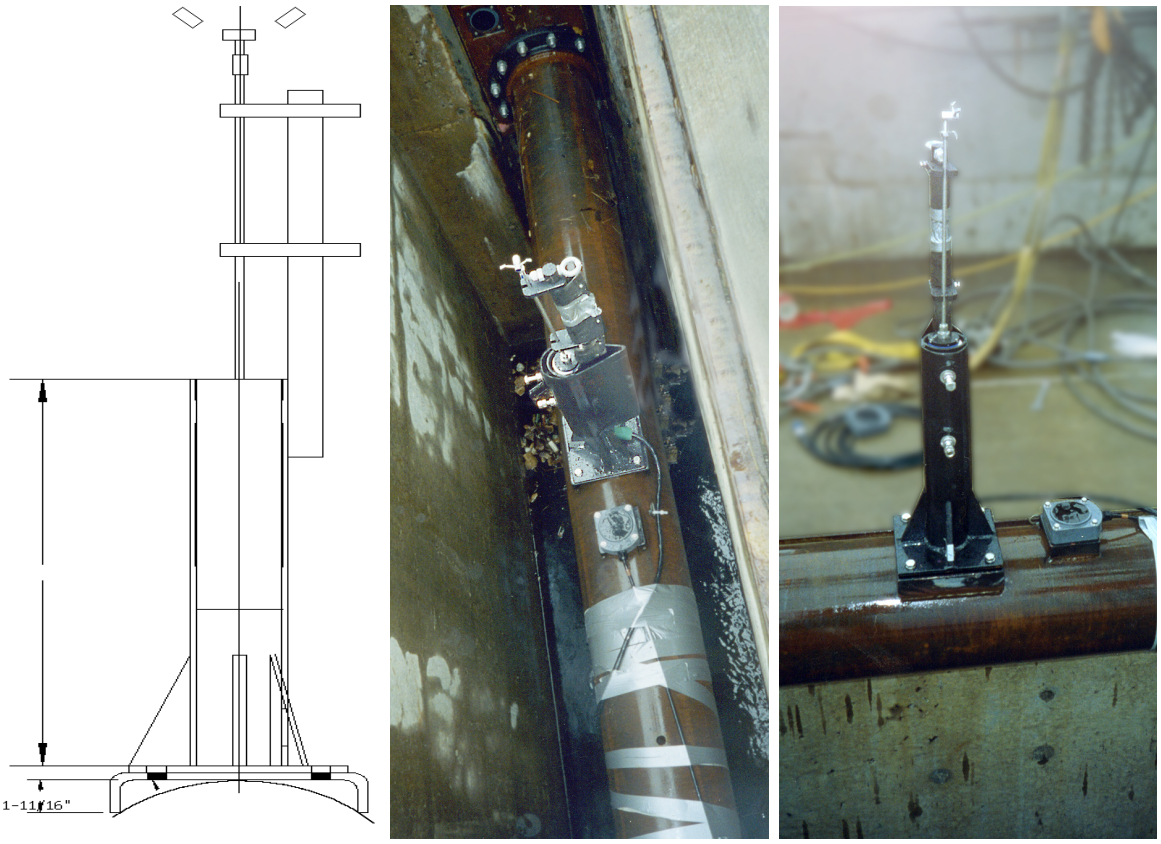

Figure 5: Left panel: Diagram of mounting arrangement for the NDV. Centre and right panels: Two views of the NDV mounted on the ASFM support frame.

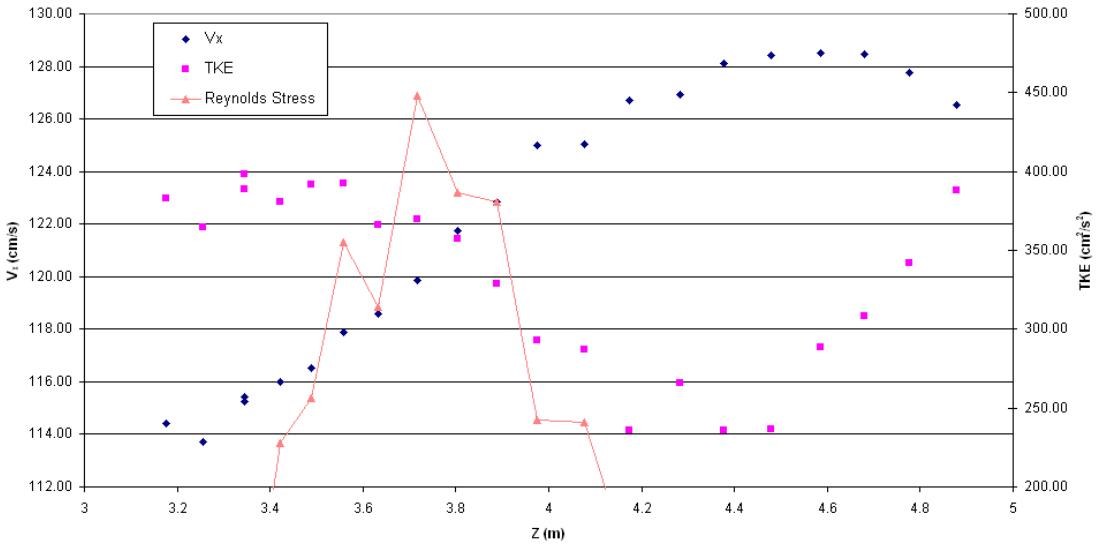

Figure 6: Profile of velocity, turbulent kinetic energy and Reynolds stress through the wake.

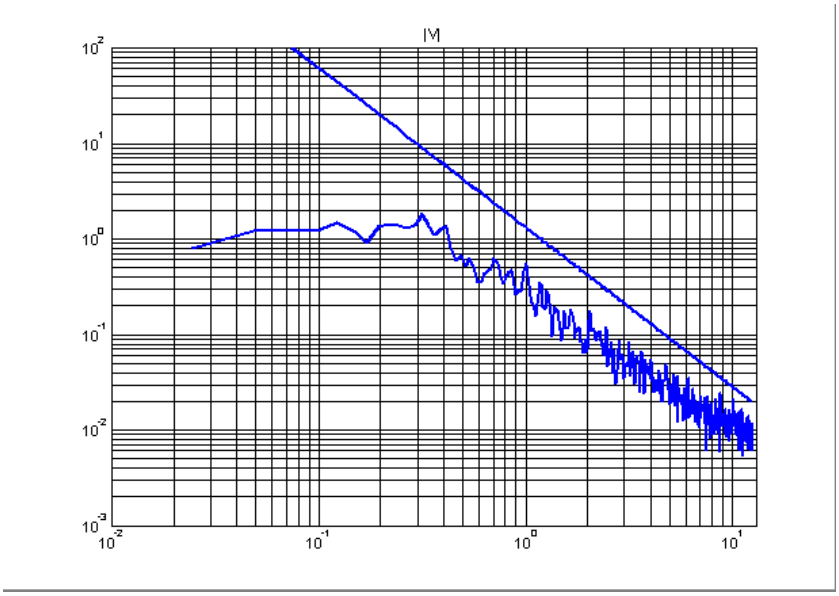

Figure 7: Power spectrum of the velocity magnitude near the wake centre. The straight line indicates a -5/3 slope.

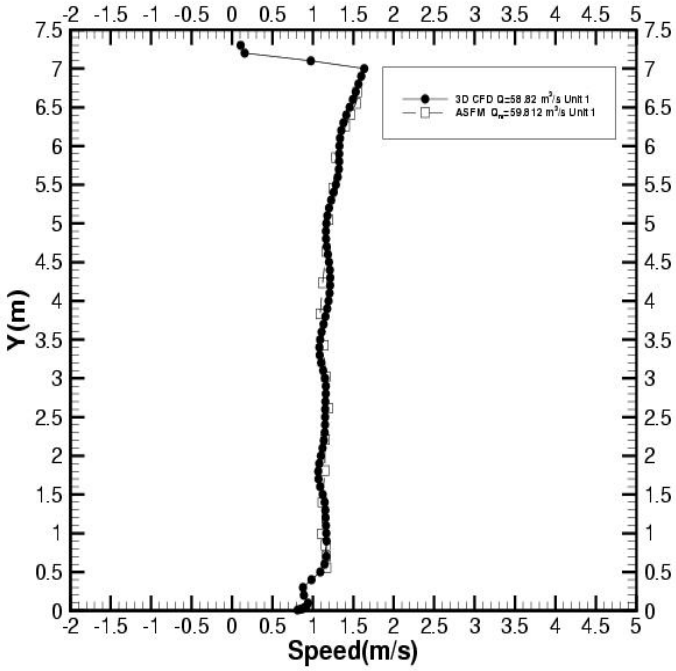

Figure 8: Comparison of the mean velocity magnitude (filled symbols) with the ASFM data (open symbols).

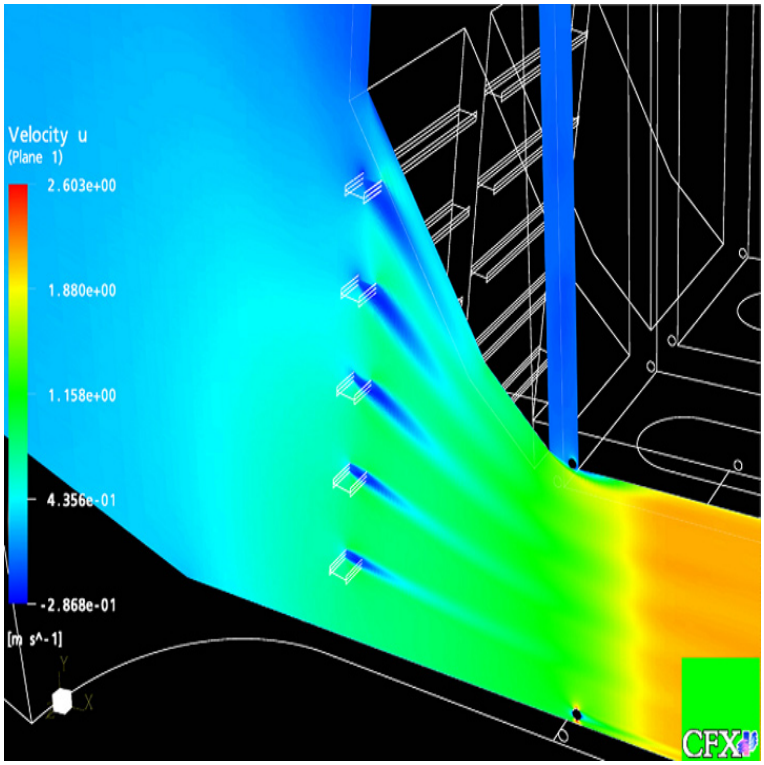

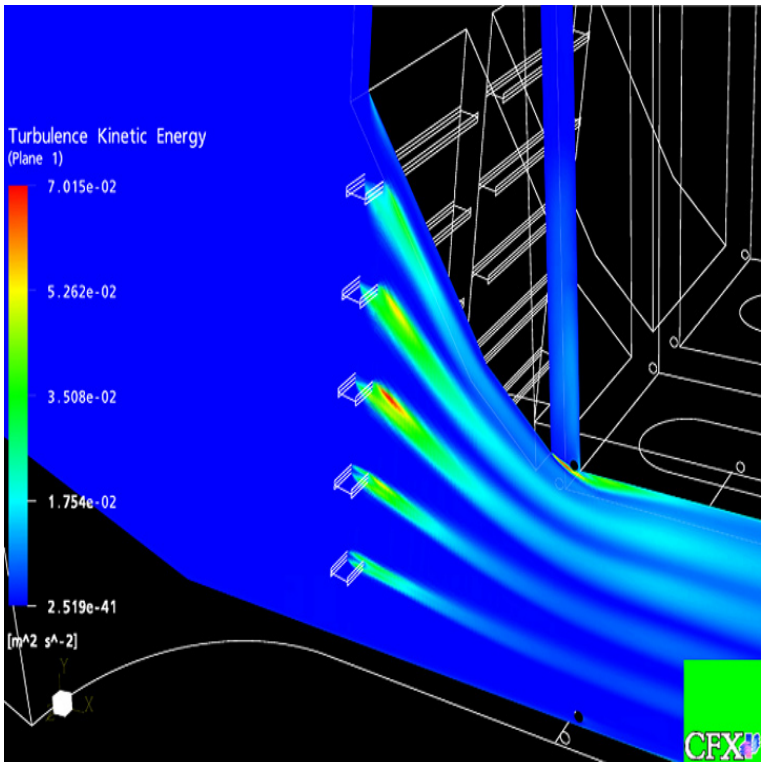

Figure 9: $\bar{U}$ velocity component and $\bar{k}$ mean turbulent kinetic energy distribution at Z=-1 m (Unit 1)

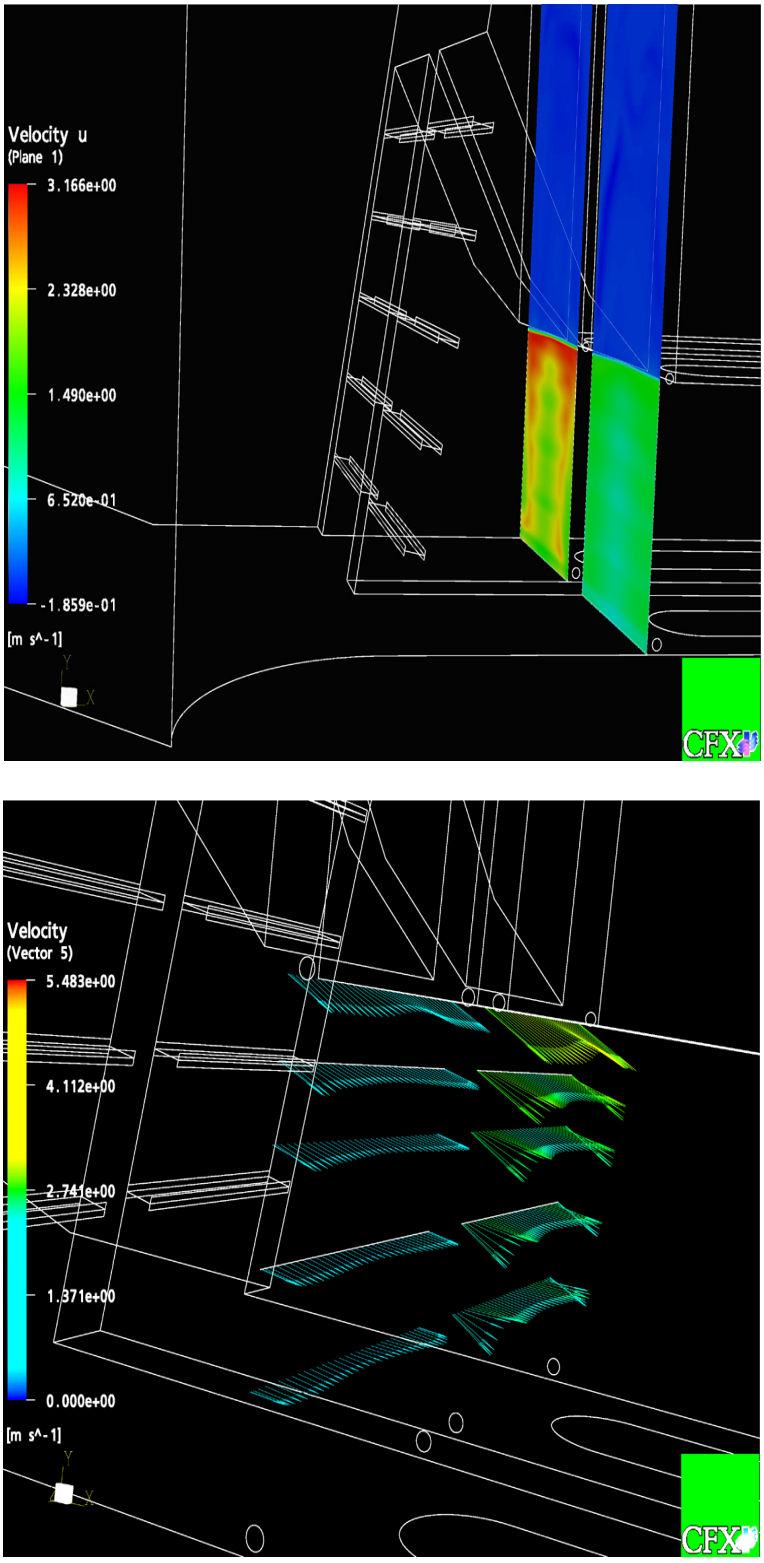

Figure 10: $\bar{U}$ velocity component distribution and selected velocity vectors in the ASFM plane.

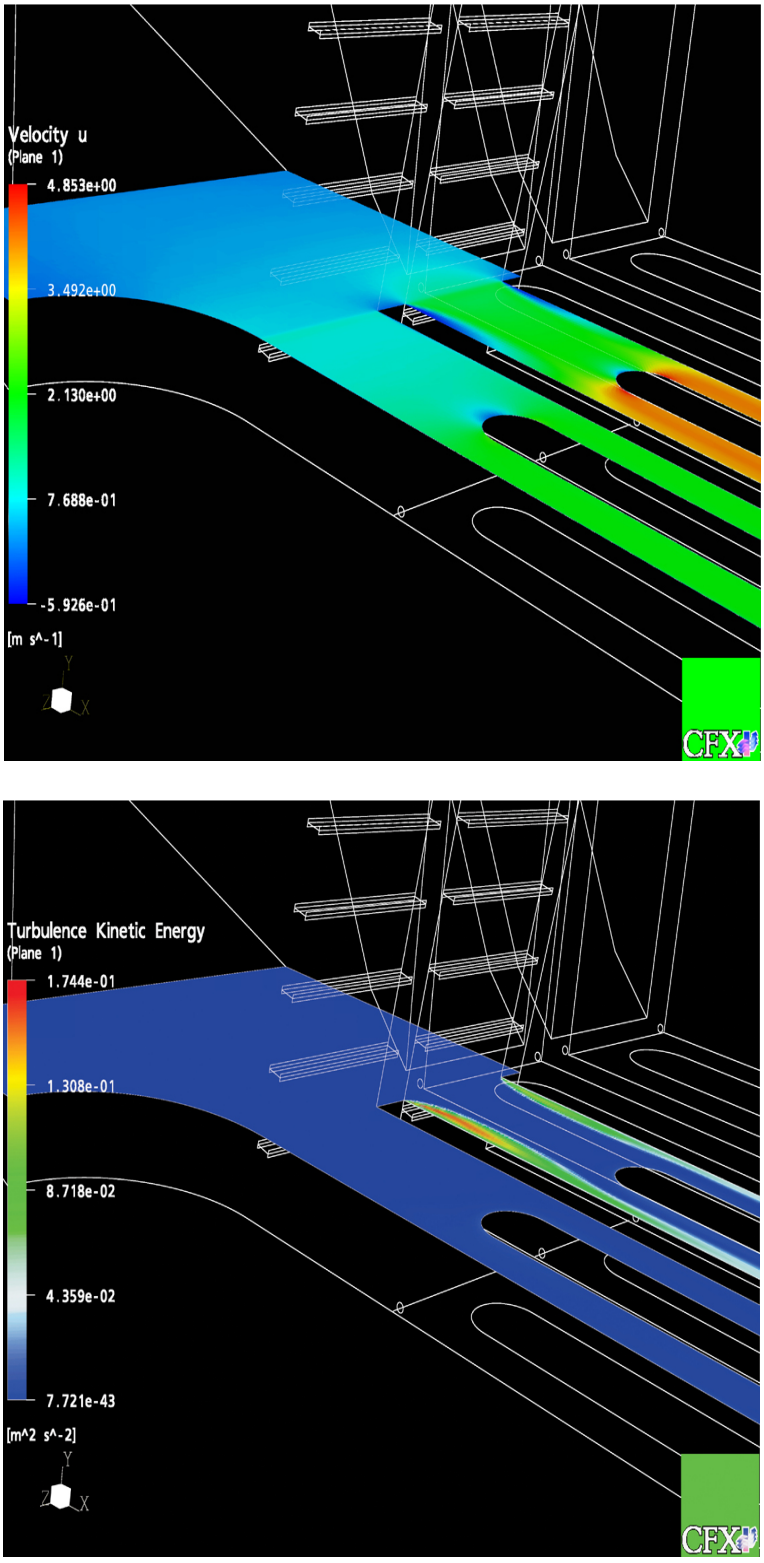

Figure 11: Cross section distribution of $\bar{U}$ and $\bar{k}$ at Y=3 m.

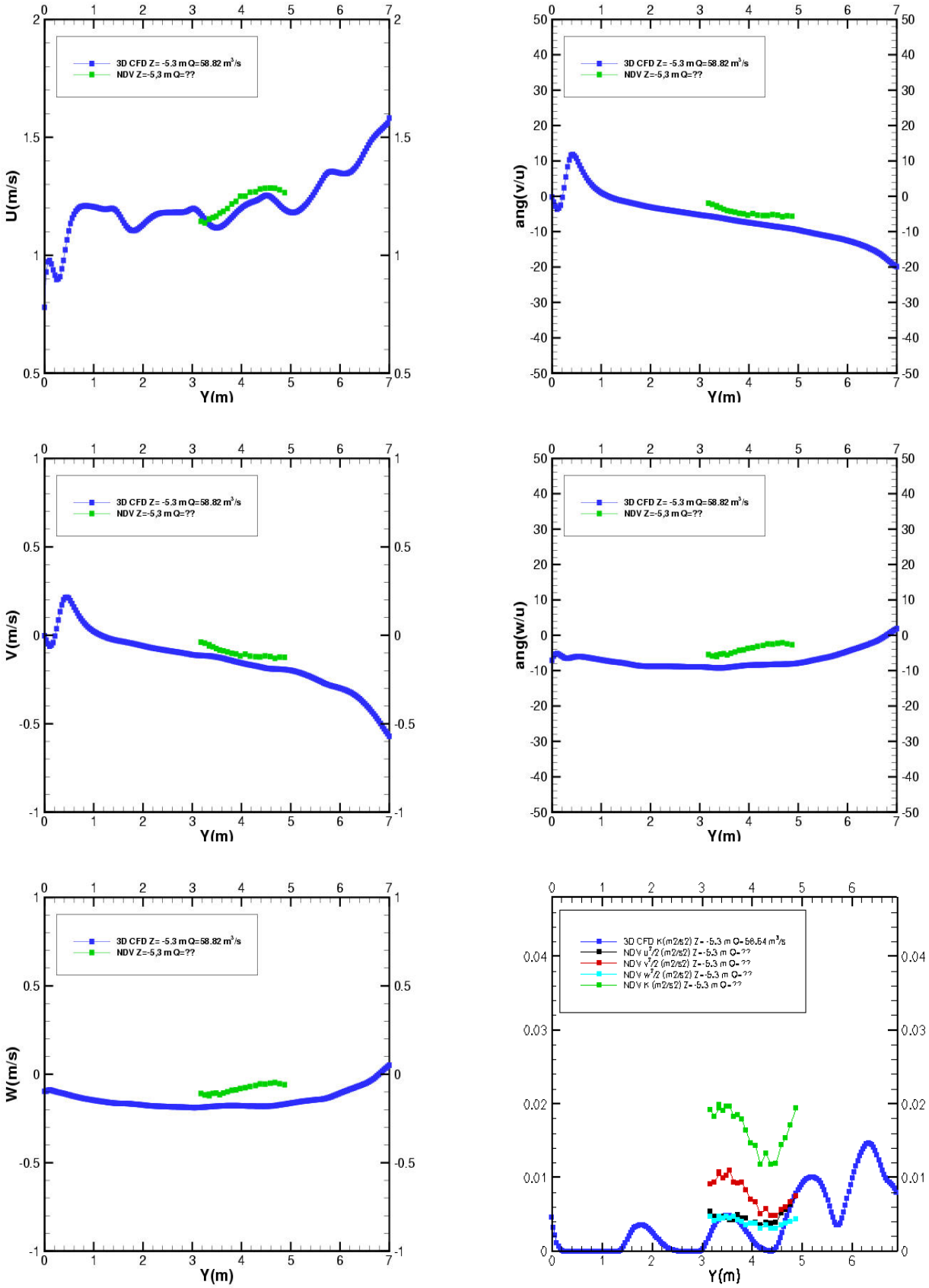

Figure 12: Comparison with the NDV measurements at (x,z)=(9 m,-5.3 m).